The Open Medicinal Chemistry Journal
DOI: 10.2174/0118741045455658260423122147, 2026, 20, e18741045455658
ISSN: 1874-1045
1

RESEARCH ARTICLE OPEN ACCESS

ROCK2 Inhibition Underlying the Anticancer Effects of Dobutamine: A Novel Proposed Mechanism

Safa Daoud[1,*], Alaa Abuawad[2], Rana Abu-Dahab[3] and Mutasem O. Taha[4,*]

[1]*Department of Pharmaceutical Chemistry and Pharmacognosy, Faculty of Pharmacy, Applied Science Private University, Amman, Jordan*
[2]*Department of Pharmaceutical Sciences and Pharmaceutics, Faculty of Pharmacy, Applied Science Private University, Amman, Jordan*
[3]*Department of Pharmaceutics and Pharmaceutical Technology, School of Pharmacy, The University of Jordan, Amman, Jordan*
[4]*Department of Pharmaceutical Sciences, School of Pharmacy, The University of Jordan, Amman, Jordan*

Abstract:

Introduction: Dobutamine, a well-established β_1-adrenergic agonist, has demonstrated anti-proliferative effects against several cancer cell types. However, the molecular mechanism underlying this activity has remained elusive. Collective evidence from the literature indicates that dobutamine-sensitive cancers-including osteosarcoma, gastric adenocarcinoma, and multiple myeloma-frequently overexpress Rho-associated protein kinase 2 (ROCK2). To evaluate the hypothesis that dobutamine can act as a ROCK2 inhibitor.

Methods: A comprehensive approach was employed, including enzymatic assays, cell-based proliferation studies in cell lines with differential ROCK2 expression, and computational molecular docking analyses.

Results: Enzyme assays demonstrated that dobutamine inhibits ROCK2 with a half-maximal inhibitory concentration (IC_{50}) of 7.1 µM. In cellular assays, dobutamine induced a ROCK2 expression-dependent anti-proliferative effect, showing approximately fourfold greater potency against the high-ROCK2-expressing HepG2 cell line compared to the low-ROCK2-expressing T-47D cell line. Furthermore, molecular docking studies revealed a plausible ATP-competitive binding mode of dobutamine within the ROCK2 kinase domain, stabilized by key hydrogen bonding, hydrophobic interactions, and π-cation interactions.

Discussion: Our findings provide the first direct evidence that dobutamine inhibits ROCK2 enzymatic activity, as demonstrated by both enzyme-based and cell-based assays. Moreover, our results validate dobutamine's chemical scaffold as a promising starting point for the structure-based design of more potent and selective ROCK2-targeted anticancer agents. Notably, we identified two major thermodynamic limitations contributing to its suboptimal binding affinity: a high entropic penalty and an enthalpic penalty associated with desolvation. Accordingly, clear medicinal chemistry optimization strategies can be employed to overcome these issues.

Conclusion: This study establishes a novel mechanistic link between dobutamine and ROCK2 inhibition, providing a strong rationale for its therapeutic repurposing.

Keywords: Dobutamine, Kinase, ROCK2, Docking, Repurposing, Hep-G2, T-47D.

*Address correspondence to these authors at the Department of Pharmaceutical Chemistry and Pharmacognosy, Faculty of Pharmacy, Applied Science Private University, Amman, Jordan and Department of Pharmaceutical Sciences, School of Pharmacy, The University of Jordan, Amman, Jordan; E-mails: s_daoud@asu.edu.jo and mutasem@ju.edu.jo

Cite as: Daoud S, Abuawad A, Abu-Dahab R, Taha M. ROCK2 Inhibition Underlying the Anticancer Effects of Dobutamine: A Novel Proposed Mechanism. Open Med Chem J, 2026; 20: e18741045455658.
http://dx.doi.org/10.2174/0118741045455658260423122147

Received: October 12, 2025
Revised: January 01, 2026
Accepted: March 18, 2026
Published: April 27, 2026

1. INTRODUCTION

The traditional de novo drug discovery and development pipeline is a challenging process, characterized by extensive timelines, prohibitive costs, and a high rate of attrition. In response to these challenges, drug repurposing-also known as drug repositioning or reprofiling-has emerged as a powerful and efficient strategy for therapeutic innovation. This approach identifies new therapeutic indications for existing drugs, capitalizing on established data regarding their safety, pharmacokinetics, and manufacturing processes to substantially shorten the bench-to-bedside trajectory [1]. The field of oncology, in particular, has been a fertile ground for drug repurposing, with numerous agents from diverse pharmacological classes being successfully repositioned to combat various malignancies [2].

Computational approaches, particularly molecular docking and machine learning-based methods, have become indispensable tools for drug repurposing, enabling rapid identification of novel drug-target interactions [3, 4]. The integration of artificial intelligence with structure-based virtual screening has proven especially valuable for kinase inhibitor repositioning, given the conserved architecture of ATP-binding pockets across the kinome [5]. The present study employs validated molecular docking protocols to complement our experimental investigations of the dobutamine-ROCK2 interaction.

Dobutamine (Fig. **1**) is a synthetic catecholamine primarily known for its clinical use as a β_1-adrenergic receptor agonist in the management of acute heart failure and cardiogenic shock [6]. Beyond its cardiovascular applications, a growing body of evidence has pointed towards unexpected anticancer properties. Seminal studies have reported that dobutamine can significantly suppress the growth of human osteosarcoma cells by inhibiting proliferation and inducing apoptosis [7]. Similarly, it has been shown to exert inhibitory effects on human gastric adenocarcinoma, impacting cell growth, colony formation, and invasion [8]. Furthermore, dobutamine has demonstrated antitumor activity against multiple myeloma cells, mediated by apoptosis induction, cell cycle arrest, and inhibition of the MAPK signaling pathway [9]. Despite these compelling phenotypic observations, the precise molecular target responsible for these anticancer effects has remained unidentified.

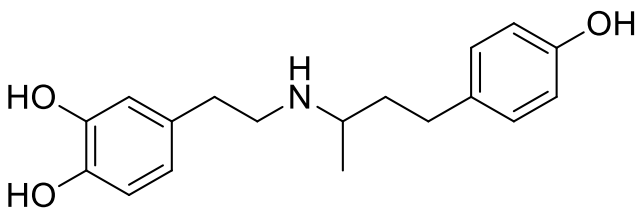

Fig. (1). Chemical structure of dobutamine.

Rho-associated protein kinase 2 (ROCK2) is a serine/threonine kinase that functions as a critical downstream effector of the RhoA GTPase. It is activated by GTP-bound RhoA, a process that is further enhanced by Polo-like kinase 1 (PLK1), which phosphorylates ROCK2 at additional sites to potentiate its activity [10, 11]. ROCK2 plays a pivotal role in regulating fundamental cellular processes, and its dysregulation is deeply implicated in cancer progression, promoting tumor proliferation, invasion, metastasis, and angiogenesis [12, 13]. A careful examination of the literature reveals that ROCK2 is not merely overexpressed but acts as an active driver of aggressive biology across the very cancer types sensitive to dobutamine, positioning it as a compelling "convergent hub" of malignancy [14, 15].

The therapeutic importance of targeting ROCK2 in oncology has gained substantial momentum in recent years. A comprehensive review by Ning *et al*. (2024) has elucidated the complex pathophysiological functions of RhoA-ROCK2 signaling in cancer progression, highlighting its role in epithelial-mesenchymal transition, migration, invasion, and therapy resistance associated with cancer stem cells [16]. Furthermore, the clinical translation of ROCK inhibitors has advanced considerably, with a recent patent review by Rodrigues de Oliveira *et al*. (2025) cataloging significant developments in ROCK inhibitor design from 2017 to 2023, underscoring the sustained pharmaceutical interest in this target class [17]. The field of kinase-targeted cancer therapy has also witnessed remarkable growth, with over 120 small-molecule kinase inhibitors now approved globally for treating various diseases, and nearly 70 FDA-approved specifically for cancer treatment as of 2024 [18]. This expanding therapeutic landscape provides a fertile context for the identification of novel ROCK2 inhibitors through drug repurposing strategies.

In osteosarcoma, ROCK2 is a key negative prognostic factor and a mediator of therapeutic resistance. Recent studies have demonstrated that elevated ROCK2 expression is associated with poor patient outcomes and drives resistance to treatments like photodynamic therapy by modulating autophagy [14, 15]. In gastric cancer, ROCK2 upregulation is correlated with increased tumor grade, invasion, and poor prognosis [19]. More recent mechanistic work has shown that ROCK2 stability is tightly regulated under hypoxic conditions and that its dysregulation is a key step in promoting epithelial-mesenchymal transition and metastasis [20]. In multiple myeloma, the therapeutic relevance of ROCK2 is well-established, with the selective ROCK2 inhibitor belumosudil demonstrating direct antimyeloma effects and enhancing the efficacy of other therapies [21]. This context is particularly relevant in the rapidly evolving treatment landscape for multiple myeloma, which now includes advanced quadruplet therapies and immunotherapies.

Recent advances have further validated ROCK2 as a promising anticancer target. Notably, Meloni *et al*. (2024) demonstrated that belumosudil exerts direct antimyeloma effects and enhances isatuximab-mediated cytotoxicity against multiple myeloma cells, providing compelling evidence for the clinical utility of ROCK2 inhibition in

hematological malignancies [21]. Concurrently, preclinical studies by Pajic *et al*. (2024) have shown that combining zelasudil, a novel selective ROCK2 inhibitor, with chemotherapy or immunotherapy significantly improves response rates in pancreatic cancer models, further expanding the potential oncologic applications of ROCK2 inhibition [21, 22].

The convergence of dobutamine's unexplained anticancer activity in specific malignancies and the established role of ROCK2 as a critical oncogenic driver in those same cancers led us to formulate a central hypothesis: Dobutamine exerts its anticancer effects, at least in part, through the direct inhibition of ROCK2. To rigorously test this hypothesis, we designed a multi-pronged investigation comprising: (i) direct enzymatic assays to quantify the inhibitory effect of dobutamine on ROCK2 kinase activity; (ii) cell-based proliferation assays using cancer cell lines with differential ROCK2 expression to link target engagement with a cellular phenotype; and (iii) *in silico* molecular docking to elucidate the structural basis of the drug-target interaction and provide a blueprint for future optimization [1, 23-25].

2. MATERIALS AND METHODS

2.1. Enzymatic Inhibition Assay

The inhibitory activities of dobutamine against ROCK2 and PLK1 were evaluated using the Z'-LYTE Kinase biochemical assay (Invitrogen, USA). Dobutamine HCl was gifted by Hikma Pharmaceuticals, Amman, Jordan (batch number: 21100697). This assay employs a fluorescence-based, coupled-enzyme format and is based on the differential sensitivity of phosphorylated and non-phosphorylated peptides to proteolytic cleavage. The peptide substrate is labeled with two fluorophores, the donor (coumarin) and the acceptor (fluorescein), which form a FRET (fluorescence resonance energy transfer) pair. When the peptide is phosphorylated, it resists proteolytic cleavage, maintaining the FRET signal. However, if the kinase is inhibited and the peptide is not phosphorylated, it becomes susceptible to cleavage, resulting in the loss of the FRET signal. This enables sensitive and reliable detection of kinase inhibition [26].

Initially, the bioactivity of dobutamine against ROCK2 and PLK1 was assessed at a single concentration of 10 µM. If the inhibitory activity was promising (*i.e*., % inhibition at 10 µM > 50%), additional concentrations were tested to determine the IC_{50} value. Each concentration was tested in duplicate. All statistical analyses were performed using GraphPad Prism (Version 9.3.1, GraphPad Software, Inc., San Diego, CA). The IC_{50} value was calculated using nonlinear regression of log (concentration) *versus* percent inhibition. Staurosporine was used as a positive control, with IC_{50} values of 2.49 nM for ROCK2 and 617.0 nM for PLK1 [26].

The Z'-LYTE platform was selected for this study based on its established reputation as an industry-standard kinase profiling technology with demonstrated reliability across more than 200 kinases [27]. This FRET-based assay offers several advantages for kinase inhibitor characterization, including ratiometric quantification that minimizes compound interference, high reproducibility, and standardized conditions that facilitate cross-study comparisons [28]. The assay has been extensively validated in drug discovery applications for both lead identification and selectivity profiling, with the SelectScreen® service being widely utilized in pharmaceutical research [29]. Internal validation was achieved using staurosporine as a positive control, which yielded IC_{50} values consistent with published literature, thereby confirming assay performance under our experimental conditions.

2.2. Cell Proliferation Assay

Hep-G2 cells (ATCC® HB-8065™) and T-47D cells (ATCC® HTB-133™), were cultured in high-glucose Dulbecco's Modified Eagle Medium (DMEM) fortified with 10% fetal bovine serum (FBS), sodium pyruvate (1 mM), 1% (v/v) L-glutamine (2 mM), 1% (v/v) penicillin (100 IU/mL) and streptomycin (100 µg/mL). Cells were seeded in 96-well plates at a density of $5.5*10^3$ cells per well and incubated in a CO_2 incubator at 37 °C. After 24 hours of seeding, dobutamine was added in a serial dilution in tissue culture media to achieve the concentrations of 250, 125, 62.5, 31.25, 15.625, 7.8125, 3.9, 1.95, and 0.485 µM. An incubation period of 72 hours followed, after which the MTT assay was carried out to assess cell viability and determine the IC_{50} values of the treatment. MTT dye was reconstituted using PBS at a 5:1 (w/v) ratio. After decanting the drugs and media, 100 µL of fresh medium in addition to 10 µL of the MTT mixture were added to each well, then the plates were incubated for 3-4 hours. The cells were examined under the microscope to ensure the formation of purple formazan crystals. Subsequently, the dye and medium were aspirated, and 100 µL/well of DMSO was added to solubilize the crystals. The plates were placed on the plate shaker for 15-20 minutes, and the absorbance was read at a wavelength of 560 nm using a microplate reader (Micro Read 1000, Global Diagnostics B, Belgium). Cell viability was calculated by comparing the absorbance of drug-treated wells to those of controls of no treatment. Each concentration was measured in quadruplicate wells, and the whole plate was repeated using at least two independent cell passages.

The MTT assay was employed as a well-established colorimetric method for assessing cell viability and proliferation, recognized for its extensive utility in cytotoxicity screening and drug discovery applications [30]. While the assay measures metabolic activity as a proxy for cell viability, careful optimization of assay parameters (cell seeding density, incubation time, and MTT concentration) was performed to ensure reliable quantification [31]. The selection of HepG2 and T-47D cell lines was based on their differential ROCK2 expression profiles as documented in the Human Protein Atlas transcriptomics database [32], providing an ideal experimental model to test the hypothesis that ROCK2 expression levels correlate with dobutamine sensitivity. This approach of comparing drug effects in cell lines with high *versus* low target expression

is a recognized strategy for phenotypic validation of target engagement [33]. Experimental reliability was ensured through quadruplicate measurements, biological replication using independent cell passages, and appropriate controls for normalization.

2.3. Molecular Docking

Searching the protein databank (https://www.rcsb.org/) identified 17 crystallographic structures of Homo sapiens ROCK2, of which only two had reasonable resolution (*i.e.*, less than 2.5 Å). The crystal structure with the lowest resolution (PDB code: 8X92, resolution 2.2 Å) was selected for the docking experiment.

The selected crystal structure was downloaded and prepared for docking using the protocol "Prepare protein" implemented in Discovery Studio (Version 4.5, Biovia Inc., USA). The following amino acids were completed and energy refined: LYS29, GLU31, ARG35, ARG38, LYS64, LYS66, ASN70, GLU76, LYS77, LYS80, LYS81, ARG100, LYS130, LYS189, LYS310, GLU374, GLU388, ASP389, and LYS401. Hydrogen atoms were added to the proteins utilizing Discovery Studio templates for protein residues. The resulting protein structures were used in subsequent docking experiments without further energy minimization. LibDock was used as a docking engine, and the binding site was defined based on the co-crystallized bound ligands, YEW.

The site-feature docking algorithm, LibDock, inserts ligands, after removing hydrogen, into a predicted active site based on binding hotspots. It aligns ligand conformations by matching their functional groups with polar and nonpolar interaction sites (hotspots) within the receptor. Ligand conformations can be generated during the docking process or pre-generated. A CHARMm minimization step can be optionally applied to refine the docked poses [34, 35].

Initially, self-docking was performed, where the co-crystallized ligand was docked into the ROCK2 binding site. Subsequently, all resulting docked poses were scored using seven scoring functions: JAIN [36], LigScore1, LigScore2 [37], PLP1 and PLP2 [38], PMF, and PMF04 [39]. The top-scoring docked poses from each of these functions were compared to the co-crystallized pose to identify the best one that could reproduce the crystal-bound pose. Self-docking was performed to select and validate the docking settings, and subsequently determine the most probable pose of dobutamine within the ROCK2 binding site.

The following LibDock parameters were used in this study: the binding site radius was set to 10.2 Å, and the docking tolerance to 0.25 Å. A total of 100 hotspots were defined. The conformation generation option was set to CAESAR, generating up to 250 conformers that did not exceed an energy threshold of 20 kcal/mol above the most stable conformer. The docking preference was set to "High Quality".

The molecular docking protocol was validated through self-docking (cognate docking) of the co-crystallized ligand YEW, a standard procedure for verifying that docking parameters and scoring functions can accurately reproduce experimentally determined binding poses [40]. The protocol was considered validated when the root mean square deviation (RMSD) between the docked pose and the crystallographic pose was below the widely accepted threshold of 2.0 Å [41, 42]. The use of multiple consensus scoring functions (JAIN, LigScore1, LigScore2, PLP1, PLP2, PMF, and PMF04) is recognized as a best practice to enhance the reliability of pose prediction and reduce scoring function bias [43]. This consensus approach has been shown to improve virtual screening performance by mitigating the limitations inherent to individual scoring functions [44].

2.4. Statistical Analysis

All statistical analyses were performed using GraphPad Prism (Version 9.3.1, GraphPad Software, Inc., San Diego, CA). For enzymatic inhibition assays, IC_{50} values were calculated by nonlinear regression fitting of log (concentration) *versus* percent inhibition using a four-parameter logistic equation; each concentration was tested in duplicate. For cell proliferation assays, each drug concentration was tested in quadruplicate wells (technical replicates), and experiments were independently repeated using at least two different cell passages (biological replicates). IC_{50} values are reported with 95% confidence intervals (CI). Statistical significance between cell lines was assessed by the non-overlapping confidence interval method [45], with $p < 0.05$ considered statistically significant. Data are presented as mean ± standard deviation (SD) where applicable.

3. RESULTS AND DISCUSSION

The conclusions of this study are supported by the convergence of three independent lines of evidence. First, biochemical assays demonstrated direct, dose-dependent inhibition of recombinant ROCK2 (IC_{50} = 7.1 µM) with a Hill slope of 0.85, consistent with well-behaved single-site inhibition. Second, cellular assays revealed a statistically significant correlation between ROCK2 expression levels and sensitivity to dobutamine's antiproliferative effects, with high-ROCK2-expressing HepG2 cells showing 3.7-fold greater sensitivity than low-ROCK2-expressing T-47D cells ($p < 0.05$). Third, molecular docking studies, validated by successful reproduction of a known co-crystal structure (RMSD = 1.27 Å), identified a plausible ATP-competitive binding mode featuring key hydrogen bonds with hinge-region residues and engagement of the catalytic lysine. Together, these data establish a novel mechanistic link between dobutamine and ROCK2 inhibition.

3.1. Dobutamine Inhibits ROCK2 Enzymatic Activity without Affecting PLK1

Drug repurposing is an attractive strategy in medicinal chemistry. While developing new drugs requires substantial investment and a long timeline, repurposing existing drugs can offer new therapeutic options using compounds that are already approved [1].

The paradigm of drug repurposing in oncology has evolved significantly in recent years, driven by advances in computational methodologies and the need for rapid therapeutic innovation. A distinctive feature of kinase inhibitors is their potential for target promiscuity, which makes them highly attractive candidates for repurposing efforts [46]. As highlighted by a recent comprehensive analysis, the promiscuous nature of kinase inhibitor binding, owing to the conserved ATP-binding pocket architecture, enables these compounds to interact with multiple kinases beyond their original intended targets, revealing unexpected therapeutic opportunities [18]. The integration of molecular docking, machine learning, and artificial intelligence has further accelerated this process, enabling computational identification of novel kinase-ligand interactions that can be rapidly validated experimentally [47].

To test our primary hypothesis, we first assessed the ability of dobutamine to directly inhibit the enzymatic activity of recombinant human ROCK2. The results demonstrated that dobutamine inhibits ROCK2 in a dose-dependent manner, yielding an IC_{50} of 7.1 µM (Fig. **2**). The dose-response curve exhibited a Hill slope of 0.85, which is consistent with a well-behaved, non-artifactual inhibition profile [48]. This finding provides the first direct evidence mechanistically linking the cardiovascular drug dobutamine to the inhibition of the oncogenic kinase ROCK2, thereby offering a plausible molecular explanation for its previously reported anticancer activities.

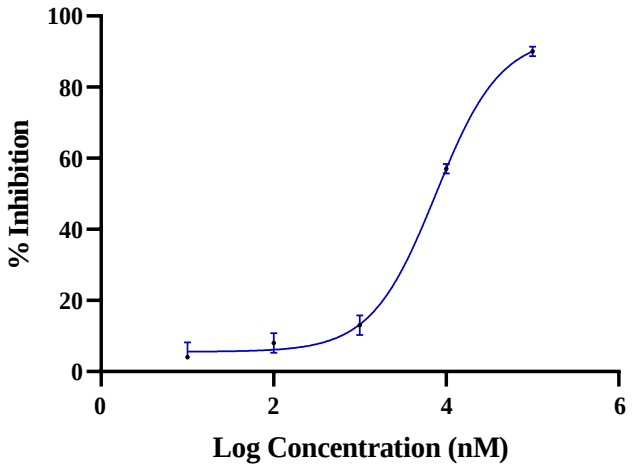

Fig. (2). Dose-response curve of dobutamine against ROCK2. Error bars represent the standard deviation of two experimental data points.

To benchmark this result, we compared dobutamine's potency against established ROCK2 inhibitors. Hydroxyfasudil (HA-1100), a well-characterized ROCK inhibitor and active metabolite of fasudil, exhibits IC_{50} values of 0.72–0.73 µM for ROCK2 [49]. The pan-ROCK inhibitor Y-27632 demonstrates IC_{50} values of 0.14–0.22 µM for both ROCK1 and ROCK2 [50]. Ripasudil (K-115), an ophthalmic ROCK inhibitor approved in Japan, shows IC_{50} values of 19 nM (0.019 µM) for ROCK2 and 51 nM (0.051 µM) for ROCK1 [51]. Belumosudil (KD025), a ROCK2-selective inhibitor recently approved by the FDA for chronic graft-versus-host disease, exhibits remarkable selectivity with an IC_{50} of 105 nM (0.105 µM) for ROCK2 *versus* 24 µM for ROCK1 [52, 53]. Thus, while dobutamine's IC_{50} of 7.1 µM is approximately 10–100-fold weaker than these dedicated ROCK inhibitors, its confirmed activity validates the scaffold for further optimization and represents a novel chemotype for this target class.

Although an IC_{50} of 7.1 µM is modest potency for a lead compound, it is still significant for a repurposed drug discovered through a hypothesis-driven approach [1, 2]. This activity is comparable to dobutamine's reported off-target inhibitory activities against other kinases, such as FYN (IC_{50} = 3.98 µM), LCK (IC_{50} = 5.52 µM), and EGFR (IC_{50} = 5.55 µM), suggesting it may act as a multi-kinase inhibitor [54]. To probe for selectivity, we also tested dobutamine against Polo-like kinase 1 (PLK1), which can activate ROCK2. At a concentration of 10 µM, dobutamine showed only 7% inhibition of PLK1, indicating a notable degree of selectivity for ROCK2 over this related kinase.

While we observed selectivity for ROCK2 over PLK1, an important consideration is the potential cross-reactivity between ROCK2 and its closely related isoform ROCK1. These two kinases share approximately 65% overall sequence identity and 92% identity within their kinase domains [55]. Although dobutamine demonstrated a clear inhibitory activity against ROCK2 through binding to the ATP-binding site, the high degree of sequence identity between the ATP-binding domains of ROCK1 and ROCK2 (≈92%) suggests that it is likely to inhibit both isoforms with similar potency. This is consistent with the behavior of other ATP-competitive ROCK inhibitors such as Y-27632, fasudil, and hydroxyfasudil, which lack selectivity between the two isoforms. Indeed, achieving ROCK2 selectivity remains a significant challenge in drug design and typically requires targeting unique structural features outside the ATP-binding pocket or exploiting allosteric sites, as exemplified by belumosudil [52, 53]. The reported off-target activities of dobutamine against other kinases (FYN, LCK, and EGFR with IC_{50} values of 3.98–5.55 µM) [54] suggest a promiscuous kinase inhibition profile that may contribute to its pleiotropic cellular effects. However, it should be noted that these IC_{50} values are within the same micromolar range as its ROCK2 activity, and the therapeutic relevance of these interactions requires further investigation in cellular and *in vivo* contexts.

3.2. Dobutamine Selectively Suppresses the Proliferation of ROCK2-Overexpressing Cells

Having established that dobutamine can directly inhibit ROCK2, we next sought to determine if this molecular activity translates into a functional cellular effect. We hypothesized that if ROCK2 is a primary intracellular target, then cells with higher levels of ROCK2 expression should be more sensitive to dobutamine's antiproliferative effects. To test this, we selected two human cancer cell lines with markedly different ROCK2

expression levels: the hepatocellular carcinoma cell line Hep-G2 (high ROCK2 expression; normalized Transcripts Per Million = 85.5) and the breast ductal carcinoma cell line T-47D (low ROCK2 expression; nTPM = 8.8) [32].

The cells were treated with increasing concentrations of dobutamine for 72 hours, and cell viability was assessed using the MTT assay. As shown in Figure **3**, dobutamine exhibited significantly greater antiproliferative potency against high-ROCK2-expressing Hep-G2 cells, with an IC_{50} of 15.2 µM (95% Confidence interval: 12.6 to 18.5). In contrast, the low-ROCK2-expressing T-47D cells were substantially less sensitive, with an IC_{50} of 56.1 µM (95% Confidence interval: 48.5 to 64.3). The difference between the two cell lines was statistically significant, with a *p*-value < 0.05, as indicated by the non-overlapping 95% confidence intervals [45]. This significant difference in potency (around 3.7 times) provides a strong correlation between cellular ROCK2 expression and sensitivity to dobutamine. This result powerfully bridges the gap between molecular target engagement and a whole-cell phenotype, providing compelling evidence that ROCK2 inhibition is a key mechanism mediating the drug's antiproliferative effects at the cellular level.

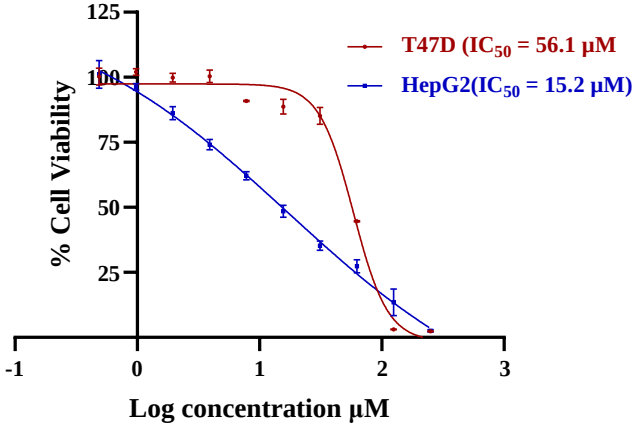

Fig. (3). Dose-dependent cytotoxicity of dobutamine in Hep-G2 and T-47D. Error bars represent the standard deviation of experimental data points (n=4).

3.3. Molecular Docking for Dobutamine in the ROCK2 Active Site

To understand the structural basis for dobutamine's inhibition of ROCK2, we performed molecular docking studies. We used the high-resolution (2.2 Å) crystal structure of human ROCK2 (PDB ID: 8X92), which was selected due to the presence of a well-defined co-crystallized ligand in the ATP-binding site, providing a high-quality receptor model. The docking protocol was first validated *via* self-docking of the co-crystallized ligand (YEW), which successfully reproduced the experimental binding pose with a root mean square deviation (RMSD) of 1.27 Å, confirming the reliability of our setup (Fig. **4**).

Dobutamine was then docked into the ROCK2 ATP-binding site. The most probable binding mode, consistently predicted by the LigScore1 and PLP1 scoring functions, is shown in (Fig. **5A** and **B**).

In order to further demonstrate the reliability of the dobutamine pose, the suggested dobutamine poses were compared to the co-crystal structures of YEW based on scores from the two valid scoring functions. Docking study demonstrated that YEW produced LigScore1 of 3.28 and PLP1 of 127.05, while dobutamine produced LigScore1 of 3.38 and PLP1 of 108.25. The fact that the LigScore1s were similar indicates that both compounds, YEW and dobutamine, would likely produce similar binding affinities for ROCK2. On the other hand, the lower score of dobutamine compared to YEW using PLP1 function correlates with experimentally derived micromolar potency of dobutamine. Accordingly. PLP1 provides a strong basis for confidence in the predicted dobutamine–ROCK2 complex. Table **1** summarizes the docking results.

It is important to note that docking scoring functions are designed primarily for pose prediction and relative compound ranking rather than absolute binding affinity prediction [4]. The correlation between docking scores and experimental IC_{50} values is inherently limited by several well-documented factors [56, 57]. First, scoring functions employ simplified representations of protein-ligand interactions that do not fully account for entropic contributions, protein flexibility, and explicit solvent effects [58]. Second, IC_{50} values represent functional inhibition under specific assay conditions and are influenced by factors beyond binding affinity, including compound solubility, assay kinetics, and ATP concentration [59]. Third, scoring functions assign fixed weights to interaction terms, whereas the actual contribution of each interaction type varies in a target-dependent and non-additive manner [56]. Consequently, while our docking results provide valuable qualitative insights into the binding mode and key interactions of dobutamine within the ROCK2 active site, a direct quantitative correlation with the experimental IC_{50} of 7.1 µM is not expected. The comparable LigScore1 values for dobutamine (3.38) and the potent reference inhibitor YEW (3.28), together with the lower PLP1 score for dobutamine (108.25 *vs*. 127.05), are qualitatively consistent with dobutamine exhibiting moderate micromolar-range inhibitory activity, supporting the validity of the predicted binding pose without implying a mathematical relationship between score magnitude and potency [37, 60].

The analysis revealed that dobutamine is anchored within the kinase domain through a network of favorable interactions. Key hydrogen bonds are formed between the catechol hydroxyl groups and the backbone of residues in the critical hinge region (Gly104, Phe103), a hallmark of ATP-competitive kinase inhibitors. Additional hydrogen bonds are formed between dobutamine's phenolic hydroxyl and the side chains of Met172 and Glu170. The molecule is further stabilized by hydrophobic contacts between its aliphatic backbone and residues such as Val106, Ala119, and Leu221, as well as a favorable electrostatic (π-cation) interaction between the electron-rich catechol ring and the positively charged side chain of Lys121.

Table 1. Comparison of docking scores of dobutamine and the co-crystallized reference ligand YEW across the validated scoring functions.

Parameter	Dobutamine	YEW (8X92)	Interpretation
LigScore1[a]	3.38	3.28	Similar values indicate comparable shape/electrostatic complementarity
PLP1[b]	108.25	127.05	Lower score for dobutamine consistent with weaker (μM *vs* nM) binding
Self-docking RMSD	N/A	1.27 Å	Protocol validated (threshold: <2.0 Å)
Experimental IC_{50}	7.1 μM	nM range	~100-fold difference in potency

Note: [a]Empirical piecewise linear potential validated for pose selection, [b]Empirical piecewise linear potential optimized for binding affinity.

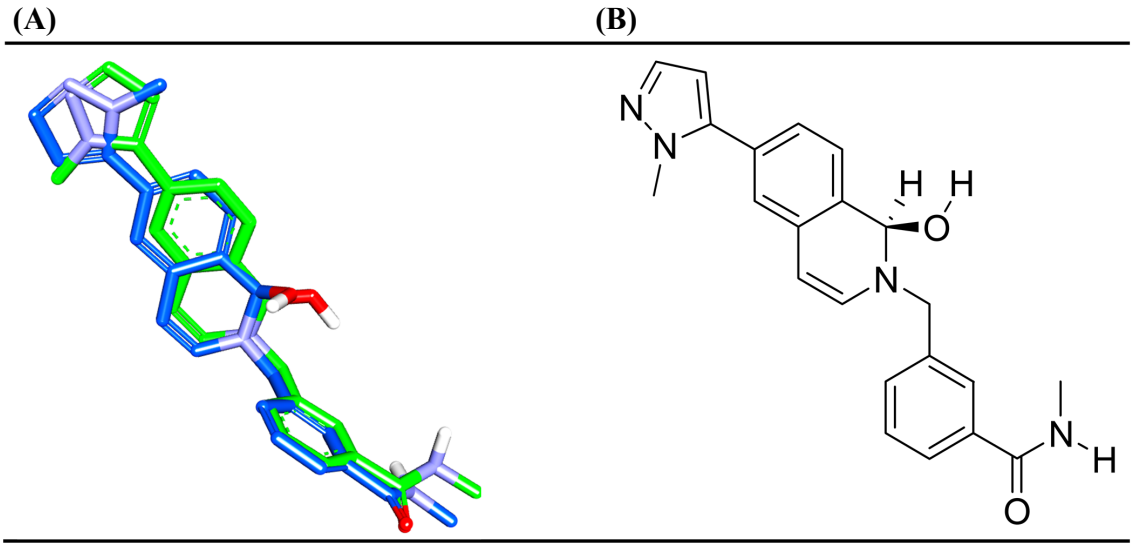

Fig. (4). (**A**) High-ranking docked poses (blue) compared to crystallographic bound pose (green) of the co-crystallized ligand, YEW (PDB code: 8X92) according to PLP1, PLP2, Jain and LigScore1. (**B**): 2D structure of the YEW.

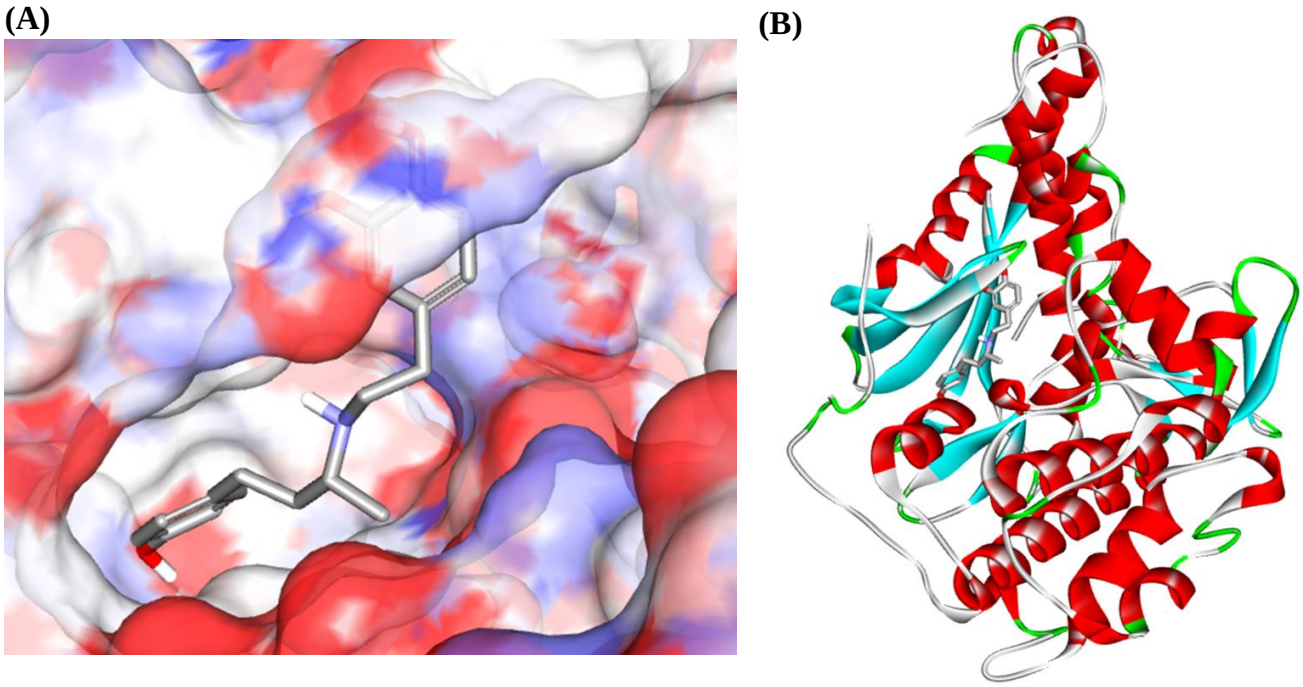

Fig. 5 contd.....

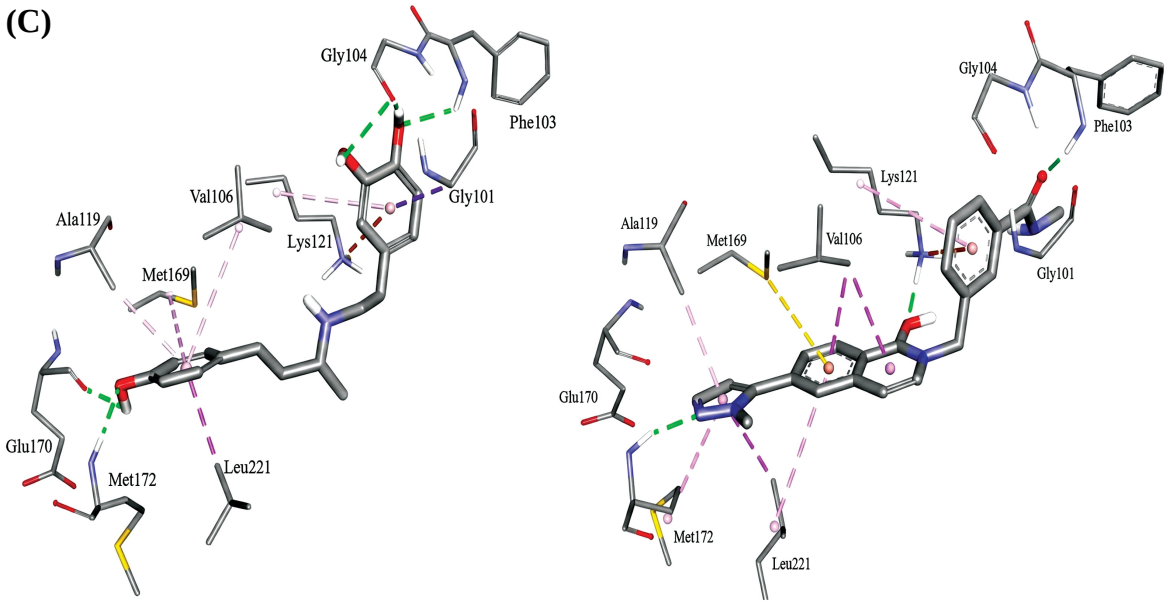

Fig. (5). The docked pose of dobutamine in ROCK2 (PDB code: 8X92, resolution 2.2 Å). (**A**): Binding site covered by a solvent-accessible surface. (**B**): Overall view of dobutamine in the binding site. (**C**): Detailed view showing the binding interactions anchoring dobutamine (left) and YEW (right) within the ROCK2 kinase binding site. Hydrogen bonds, hydrophobic, and electrostatic attractive interactions are shown as green, purple and orange dotted lines, respectively.

Based on the docking analysis and comparison with established ROCK inhibitor pharmacophores, the essential functional groups of dobutamine for ROCK2 inhibition can be identified [61, 62], as in Table **2**. The phenol moiety represents the primary pharmacophoric element, functioning as a hinge-binding scaffold analogous to the indazole, pyrazole, and isoquinoline moieties employed by approved ROCK inhibitors such as belumosudil and fasudil [63]. This hydroxyl provides both hydrogen bond donor and acceptor capabilities essential for engaging the kinase hinge backbone, a conserved feature across ATP-competitive kinase inhibitors [64]. It hydrogen bonds with Met172 and Glu170 residues that have been identified as key determinants of ROCK2 inhibitor potency in prior SAR studies [65]. The catechol hydroxyls, on the other hand, seem to engage in hydrogen bonding with Phe103 and Gly104 of the glycine-rich loop, further stabilizing the binding interaction. In contrast, the secondary amine within the aliphatic linker, while contributing to overall molecular polarity, does not form direct hydrogen bonds with the protein and is positioned in a solvent-exposed region adjacent to the hydrophobic residue Val106. This observation suggests that the amine represents a potential site for structural modification to reduce desolvation penalties without compromising target engagement. The aliphatic chain connecting the two aromatic systems provides conformational flexibility and enables hydrophobic contacts with Val106, Ala119, and Leu221, though the entropic cost of constraining this flexible linker upon binding likely contributes to the modest micromolar potency observed [66].

Table 2. Summary of dobutamine–ROCK2 interactions.

Interaction Type[a]	ROCK2 Residue	Protein Atom/Group	Dobutamine Functional Group	Distance (Å)	Functional Role
Hydrogen Bond	Gly104	Backbone C=O	3-OH (catechol)	2.8–3.2	(GK+1)[b]
Hydrogen Bond	Phe103	Backbone N–H	4-OH (catechol)	2.8–3.2	(GK+3)
Hydrogen Bond	Met172	Side chain S	para-OH (phenyl)	3.0–3.5	ROCK2 specificity
Hydrogen Bond	Glu170	Side chain COO^-	para-OH (phenyl)	2.6–3.0	ROCK2 specificity
π-Cation	Lys121	Side chain NH_3^+	Catechol ring	3.5–4.5	Catalytic lysine engagement
Hydrophobic	Val106	Side chain (isopropyl)	Aliphatic linker	3.5–4.0	Pocket filling
Hydrophobic	Ala119	Side chain (methyl)	Aliphatic linker	3.5–4.0	Pocket filling
Hydrophobic	Leu221	Side chain (isobutyl)	Aliphatic linker	3.5–4.0	Pocket filling

Note: [a]**Distance Ranges:** Hydrogen bonds: 2.5–3.5 Å (heavy atom distances); π-Cation interactions: 3.5–4.5 Å (cation to ring centroid); Hydrophobic contacts: 3.5–4.0 Å (van der Waals contact distance). [b]**Nomenclature:** GK = Gatekeeper residue, GK+1, GK+3 = Residues downstream from gatekeeper that form canonical hinge interactions. ATP-competitive inhibitors characteristically form 1–3 hydrogen bonds with these residues.

Table 3. Comparison of key interactions: dobutamine *vs.* reference ROCK2 inhibitor.

Interaction	Dobutamine	YEW (PDB code: 8X92)
GK+1 / H-bond 1	Gly104 (C=O)	No H-bond with Gly104
GK+3 / H-bond 2	Phe103 (N-H)	Phe103 (N-H)
Met172 contact	Yes (H-bond)	Yes (H-bond)
Glu170 contact	Yes (H-bond)	No (H-bond)
Lys121 interaction	π-cation	π-cation /H-bond
Hydrophobic contacts	Val106, Ala119, Leu221	Val106, Ala119, Leu221
Hinge-binding moiety	Phenol	Indazole
Experimental IC_{50}	7.1 μM	nM (potent)

Note: Nomenclature: GK = Gatekeeper residue, GK+1, GK+3 = Residues downstream from gatekeeper that form canonical hinge interactions. ATP-competitive inhibitors characteristically form 1–3 hydrogen bonds with these residues.

Table **3** and Figure **5C** compare dobutamine's predicted binding interactions within the ROCK2 ATP-binding site with those of the co-crystallized ligand YEW (PDB ID: 8X92). The two compounds exhibit striking similarity in their interaction profiles, sharing hydrogen bonds with critical residue Phe103, contacts with ROCK2-specificity determinants (Met172, Glu170), and hydrophobic interactions with the adenine pocket (Val106, Ala119, Leu221). This pharmacophoric conservation validates dobutamine's predicted binding mode despite its structurally distinct catechol scaffold.

While the docked pose reveals several favorable interactions, the modest binding affinity (IC_{50} = 7.1 μM) can be rationalized from a structural and thermodynamic perspective. The significant conformational flexibility of dobutamine's aliphatic chain, which contains multiple rotatable bonds, incurs a substantial entropic cost upon adopting the constrained, bioactive conformation required for binding [67, 68]. Furthermore, the presence of four polar functional groups (three hydroxyls and one amine) necessitates a significant enthalpic penalty for desolvation prior to entering the relatively hydrophobic ATP-binding pocket [69, 70].

Importantly, the predicted ATP-competitive binding mode, centered on the highly conserved kinase hinge region, suggests that dobutamine is unlikely to possess significant selectivity for ROCK2 over the closely related ROCK1 isoform. The ATP-binding sites of these two kinases are nearly identical, and achieving selectivity typically requires exploiting subtle differences in peripheral regions or targeting allosteric sites. This represents a key challenge for the future development of this scaffold, as ROCK2 selectivity is a primary goal in modern inhibitor design to mitigate potential side effects associated with pan-ROCK inhibition.

3.4. Dobutamine as a Lead Scaffold for Next-Generation ROCK2 Inhibitors

The docking model not only provides a rationale for dobutamine's activity but also serves as a valuable base for structure-based drug design aimed at improving its potency and selectivity. Based on the identified structural and thermodynamic liabilities, a clear medicinal chemistry optimization strategy can be proposed.

To address the high entropic penalty associated with binding [67, 68], rigidification of the scaffold is paramount. This could be achieved by incorporating the flexible butylamine chain into a cyclic system, such as a piperidine or pyrrolidine ring. Such a modification would pre-organize the molecule into a lower-energy bioactive conformation, reducing the entropic cost of binding and potentially enhancing affinity.

To tackle the enthalpic penalty of desolvation [69, 70], modifications to reduce polarity are necessary. The docking pose (Fig. **5**) indicates that the secondary amine is solvent-exposed and surrounded by lipophilic residue (Val106). As this moiety does not form key hydrogen bonds, it could be replaced with a less polar group (*e.g.*, an ether linkage) or incorporated into a heterocyclic ring to reduce the desolvation penalty without disrupting essential interactions.

While dobutamine's potency is modest compared to dedicated, novel ROCK2 inhibitors like Zelasudil (RXC007) [23] or newly discovered pyrazolone-based scaffolds [71], its established clinical safety profile and novel chemotype for this target class make it a valuable starting point. This study successfully validates the dobutamine scaffold for ROCK2 inhibition, providing a solid foundation for future structure-based design campaigns. Such campaigns can now rationally pursue the development of potent and, crucially, selective ROCK2 inhibitors for oncologic indications.

Importantly, as an FDA-approved medication with over four decades of clinical use, dobutamine possesses a well-characterized safety and pharmacokinetic profile that can be leveraged in repurposing efforts [1]. The ROCK2-expression-dependent antiproliferative activity observed in this study-with HepG2 cells (high ROCK2 expression) exhibiting 3.7-fold greater sensitivity than T-47D cells (low ROCK2 expression)-suggests that the observed effects are target-mediated rather than indicative of indiscriminate cytotoxicity. This mechanistic selectivity, combined with dobutamine's established clinical tolerability, supports further investigation of its potential as a ROCK2-targeted anticancer agent in appropriate preclinical models.

Our findings add dobutamine to the growing list of cardiovascular drugs with demonstrated anticancer

potential. This expanding class includes propranolol, which exhibits anti-metastatic effects through β-adrenergic receptor blockade and is currently in clinical trials for multiple cancer types [72]; carvedilol, which suppresses osteosarcoma and breast cancer cell viability through growth factor receptor interference [73]; and losartan, which normalizes the tumor microenvironment by reducing stromal fibrosis [74]. Unlike these agents, which primarily exert their effects through modulation of adrenergic, angiotensin, or ion channel signaling, dobutamine appears to act through direct kinase inhibition-specifically, ROCK2. This mechanistic distinction positions dobutamine as a unique addition to the cardiovascular-to-oncology repurposing paradigm and suggests that systematic screening of cardiovascular drugs against kinase panels may reveal additional repurposing opportunities.

4. STUDY LIMITATIONS

Several limitations of this study should be acknowledged. The enzymatic IC_{50} of 7.1 μM represents modest potency that would require significant optimization for therapeutic application. ROCK1/ROCK2 selectivity was not experimentally determined, and given the highly conserved ATP-binding sites between these isoforms (92% sequence identity within the kinase domain), dobutamine likely functions as a pan-ROCK inhibitor. The cellular studies were limited to two cancer cell lines, and broader validation across additional ROCK2-dependent cancer models is warranted. Furthermore, *in vivo* efficacy and pharmacokinetic considerations were not addressed, and the relative contribution of ROCK2 inhibition *versus* β-adrenergic receptor modulation to dobutamine's cellular effects was not deconvoluted in this study.

CONCLUSION

This study provides the first direct evidence that the cardiovascular drug dobutamine inhibits ROCK2 kinase activity, offering a mechanistic explanation for its previously reported anticancer effects. Biochemical assays demonstrated that dobutamine inhibits recombinant human ROCK2 with an IC_{50} of 7.1 μM and a Hill slope of 0.85, consistent with well-behaved, single-site inhibition. This molecular activity translated to a ROCK2-expression-dependent cellular phenotype, with dobutamine exhibiting 3.7-fold greater antiproliferative potency against high-ROCK2-expressing HepG2 cells (IC_{50} = 15.2 μM) compared to low-ROCK2-expressing T-47D cells (IC_{50} = 56.1 μM; $p < 0.05$). Molecular docking studies revealed that dobutamine occupies the ATP-binding site of ROCK2, forming hydrogen bonds with hinge-region residues (Gly104, Phe103) and ROCK2-specificity determinants (Met172, Glu170), providing a structural rationale for the observed inhibitory activity. Structure-activity relationship analysis identified the catechol moiety and para-hydroxyl group as essential pharmacophoric elements responsible for target engagement, while the secondary amine and flexible aliphatic linker were identified as structural liabilities contributing to modest potency through desolvation penalties and entropic costs, respectively.

These findings establish dobutamine as a novel chemical scaffold for ROCK2 inhibition, structurally distinct from approved inhibitors such as belumosudil and fasudil, and provide a validated binding pose that can serve as a blueprint for rational optimization campaigns. These findings are particularly timely given the growing recognition of RhoA-ROCK2 signaling as a critical driver of cancer progression and therapeutic resistance, and the expanding role of kinase-targeted therapies in oncology. This work demonstrates the utility of hypothesis-driven computational approaches in drug repurposing, particularly for kinase targets where conserved binding site architecture facilitates the identification of unexpected drug-target interactions.

Future investigations should focus on medicinal chemistry optimization to improve potency through scaffold rigidification and polarity reduction at the identified liability sites, experimental determination of ROCK1/ROCK2 selectivity, validation in additional cancer models with characterized ROCK2 dependency, and *in vivo* efficacy studies to assess therapeutic potential. In summary, this study establishes a novel mechanistic link between dobutamine and ROCK2 inhibition, providing both a rationale for its anticancer effects and a foundation for the development of improved ROCK2-targeted agents.

AUTHORS' CONTRIBUTIONS

The authors confirm contribution to the paper as follows: S.D.: Conceptualization, investigation, writing; A.A.: Analysis, review & editing; R.A.: Investigation, writing; M.O.T.: Conceptualization, review & editing, supervision. All authors have read and agreed to the published version of the manuscript.

LIST OF ABBREVIATIONS

ROCK2	=	Rho-associated Protein Kinase 2
PLK1	=	Polo-Like Kinase 1
FRET	=	Fluorescence Resonance Energy Transfer
DMEM	=	Dulbecco's Modified Eagle Medium
SD	=	Standard Deviation
CI	=	Confidence Intervals

ETHICS APPROVAL AND CONSENT TO PARTICIPATE

Not applicable.

HUMAN AND ANIMAL RIGHTS

Not applicable.

CONSENT FOR PUBLICATION

Not applicable.

AVAILABILITY OF DATA AND MATERIALS

The data and supportive information is available within the article.

FUNDING

This research was funded by the Applied Science Private University, Amman, Jordan, Grant Number: DRGS/2025/7.

CONFLICT OF INTEREST

The authors declare no conflict of interest, financial or otherwise.

ACKNOWLEDGEMENTS

The authors thank the Deanships of Scientific Research at Applied Sciences Private University (Amman) and the University of Jordan for sponsoring this project.

REFERENCES

[1] Pushpakom, S.; Iorio, F.; Eyers, P.A.; Escott, K.J.; Hopper, S.; Wells, A.; Doig, A.; Guilliams, T.; Latimer, J.; McNamee, C.; Norris, A.; Sanseau, P.; Cavalla, D.; Pirmohamed, M. Drug repurposing: Progress, challenges and recommendations. *Nat. Rev. Drug Discov.,* **2019**, *18*(1), 41-58. http://dx.doi.org/10.1038/nrd.2018.168 PMID: 30310233

[2] Al Khzem, A.H.; Gomaa, M.S.; Alturki, M.S.; Tawfeeq, N.; Sarafroz, M.; Alonaizi, S.M.; Al Faran, A.; Alrumaihi, L.A.; Alansari, F.A.; Alghamdi, A.A. Drug repurposing for cancer treatment: A comprehensive review. *Int. J. Mol. Sci.,* **2024**, *25*(22), 12441. http://dx.doi.org/10.3390/ijms252212441 PMID: 39596504

[3] Pinzi, L.; Rastelli, G. Molecular docking: Shifting paradigms in drug discovery. *Int. J. Mol. Sci.,* **2019**, *20*(18), 4331. http://dx.doi.org/10.3390/ijms20184331 PMID: 31487867

[4] Ain, Q.U.; Aleksandrova, A.; Roessler, F.D.; Ballester, P.J. Machine-learning scoring functions to improve structure-based binding affinity prediction and virtual screening. *Wiley Interdiscip. Rev. Comput. Mol. Sci.,* **2015**, *5*(6), 405-424. http://dx.doi.org/10.1002/wcms.1225 PMID: 27110292

[5] Réau, M.; Langenfeld, F.; Zagury, J.F.; Lagarde, N.; Montes, M. Decoys selection in benchmarking datasets: Overview and perspectives. *Front. Pharmacol.,* **2018**, *9*, 11. http://dx.doi.org/10.3389/fphar.2018.00011 PMID: 29416509

[6] Broberg, O.; Øra, I.; Weismann, C.G.; Wiebe, T.; Liuba, P. Childhood cancer survivors have impaired strain-derived myocardial contractile reserve by dobutamine stress echocardiography. *J. Clin. Med.,* **2023**, *12*(8), 2782. http://dx.doi.org/10.3390/jcm12082782 PMID: 37109119

[7] Yin, J.; Dong, Q.; Zheng, M.; Xu, X.; Zou, G.; Ma, G.; Li, K. Antitumor activity of dobutamine on human osteosarcoma cells. *Oncol. Lett.,* **2016**, *11*(6), 3676-3680. http://dx.doi.org/10.3892/ol.2016.4479 PMID: 27284371

[8] Zheng, H.X.; Wu, L-N.; Xiao, H.; Du, Q.; Liang, J-F. Inhibitory effects of dobutamine on human gastric adenocarcinoma. *World J. Gastroenterol.,* **2014**, *20*(45), 17092-17099. http://dx.doi.org/10.3748/wjg.v20.i45.17092 PMID: 25493021

[9] Xie, B.; Xu, Z.; Yang, G.; Chen, G.; Li, B.; Hu, L.; Xiao, W.; Sun, X.; Gao, M.; Gao, L.; Wu, X.; Tao, Y.; Zhu, W.; Shi, J. Antitumor effect of dobutamine on multiple myeloma *via* mitogen-activated protein kinase pathway *in vitro*. *Acta Biochim. Biophys. Sin.,* **2016**, *48*(12), 1135-1137. http://dx.doi.org/10.1093/abbs/gmw110 PMID: 27797722

[10] Hartmann, S.; Ridley, A.J.; Lutz, S. The function of Rho-associated kinases ROCK1 and ROCK2 in the pathogenesis of cardiovascular disease. *Front. Pharmacol.,* **2015**, *6*, 276. http://dx.doi.org/10.3389/fphar.2015.00276 PMID: 26635606

[11] Lowery, D.M.; Clauser, K.R.; Hjerrild, M.; Lim, D.; Alexander, J.; Kishi, K.; Ong, S.E.; Gammeltoft, S.; Carr, S.A.; Yaffe, M.B. Proteomic screen defines the Polo-box domain interactome and identifies Rock2 as a Plk1 substrate. *EMBO J.,* **2007**, *26*(9), 2262-2273. http://dx.doi.org/10.1038/sj.emboj.7601683 PMID: 17446864

[12] Wei, L.; Surma, M.; Shi, S.; Lambert-Cheatham, N.; Shi, J. Novel insights into the roles of Rho kinase in cancer. *Arch. Immunol. Ther. Exp.,* **2016**, *64*(4), 259-278. http://dx.doi.org/10.1007/s00005-015-0382-6 PMID: 26725045

[13] Vigil, D.; Kim, T.Y.; Plachco, A.; Garton, A.J.; Castaldo, L.; Pachter, J.A.; Dong, H.; Chen, X.; Tokar, B.; Campbell, S.L.; Der, C.J. ROCK1 and ROCK2 are required for non-small cell lung cancer anchorage-independent growth and invasion. *Cancer Res.,* **2012**, *72*(20), 5338-5347. http://dx.doi.org/10.1158/0008-5472.CAN-11-2373 PMID: 22942252

[14] Zucchini, C.; Manara, M.C.; Cristalli, C.; Carrabotta, M.; Greco, S.; Pinca, R.S.; Ferrari, C.; Landuzzi, L.; Pasello, M.; Lollini, P.L.; Gambarotti, M.; Donati, D.M.; Scotlandi, K. ROCK2 deprivation leads to the inhibition of tumor growth and metastatic potential in osteosarcoma cells through the modulation of YAP activity. *J. Exp. Clin. Cancer Res.,* **2019**, *38*(1), 503. http://dx.doi.org/10.1186/s13046-019-1506-3 PMID: 31878963

[15] Deng, X.; Yi, X.; Huang, D.; Liu, P.; Chen, L.; Du, Y.; Hao, L. ROCK2 mediates osteosarcoma progression and TRAIL resistance by modulating O-GlcNAc transferase degradation. *Am. J. Cancer Res.,* **2020**, *10*(3), 781-798. http://dx.doi.org/10.1038/s41467-018-07461-x PMID: 32266091

[16] Ning, Y.; Zheng, M.; Zhang, Y.; Jiao, Y.; Wang, J.; Zhang, S. RhoA-ROCK2 signaling possesses complex pathophysiological functions in cancer progression and shows promising therapeutic potential. *Cancer Cell Int.,* **2024**, *24*(1), 339. http://dx.doi.org/10.1186/s12935-024-03519-7 PMID: 39402585

[17] de Oliveira, D.R.; Tolomeu, H.V.; Manssour Fraga, C.A.; Moreira Lima, L. Rho kinase inhibitors: A patent review (2017–2023). *Expert Opin. Ther. Pat.,* **2025**, *35*(8), 811-837. http://dx.doi.org/10.1080/13543776.2025.2522735 PMID: 40552832

[18] Li, J.; Gong, C.; Zhou, H.; Liu, J.; Xia, X.; Ha, W.; Jiang, Y.; Liu, Q.; Xiong, H. Kinase inhibitors and kinase-targeted cancer therapies: Recent advances and future perspectives. *Int. J. Mol. Sci.,* **2024**, *25*(10), 5489. http://dx.doi.org/10.3390/ijms25105489 PMID: 38791529

[19] Li, M.; Ke, J.; Wang, Q.; Qian, H.; Yang, L.; Zhang, X.; Xiao, J.; Ding, H.; Shan, X.; Liu, Q.; Xiao, Y.; Bao, B.; Huang, H. Upregulation of ROCK2 in gastric cancer cell promotes tumor cell proliferation, metastasis and invasion. *Clin. Exp. Med.,* **2017**, *17*(4), 519-529. http://dx.doi.org/10.1007/s10238-016-0444-z PMID: 27921230

[20] Yu, Z.; Pan, T.; Wang, X.; Jin, Z.; Lu, Y.; Wu, X.; Hou, J.; Wu, A.; Li, Z.; Chang, X.; Zhou, Q.; Li, J.; Liu, W.; Ni, Z.; Yang, Z.; Li, C.; Yan, M.; Liu, B.; Yan, C.; Zhu, Z.; Su, L. Loss of DRD5P2 in hypoxia attenuates Rock2 degradation to promote EMT and gastric cancer metastasis. *Biochim. Biophys. Acta Mol. Basis Dis.,* **2025**, *1871*(6), 167858. http://dx.doi.org/10.1016/j.bbadis.2025.167858 PMID: 40280198

[21] Meloni, M.; Perrin, P.; Nouguier, C.; Poirier, S.; Bouaboula, M.; Bisht, K.; de Velde, H.V.; Virone-Oddos, A.; Chiron, M. Abstract 5277: The ROCK-2 inhibitor belumosudil exerts a direct antimyeloma effect and improves isatuximab-mediated cytotoxicity against multiple myeloma cells. *Cancer Res.,* **2024**, *84*(6_Supplement)(Suppl.), 5277. http://dx.doi.org/10.1158/1538-7445.AM2024-5277

[22] Pajic, M.; McLean, B.; Fajardo, D.C.; Porazinski, S.; Upton, D.H.; Schuhmacher, D.; Istadi, A.; Cox, T.; Timpson, P.; Wilcock, D.J.; Anderson, K.J.; Mason, H.; Guisot, N.E.; Jones, C.D.; Phillips, C.; Armer, R. Abstract 720: Combining zelasudil, a small molecule ROCK2 inhibitor, with chemotherapy or immunotherapy improves response in preclinical models of pancreatic cancer. *Cancer Res.,* **2024**, *84*(6_Supplement)(Suppl.), 720. http://dx.doi.org/10.1158/1538-7445.AM2024-720

[23] Pereira Moreira, B.; Weber, M.H.W.; Haeberlein, S.; Mokosch,

A.S.; Spengler, B.; Grevelding, C.G.; Falcone, F.H. Drug repurposing and de novo drug discovery of protein kinase inhibitors as new drugs against schistosomiasis. *Molecules,* **2022**, *27*(4), 1414. http://dx.doi.org/10.3390/molecules27041414 PMID: 35209202

[24] Daoud, S.; Alabed, S.J.; Dahabiyeh, L.A. Identification of potential COVID-19 main protease inhibitors using structure-based pharmacophore approach, molecular docking and repurposing studies. *Acta Pharm.,* **2021**, *71*(2), 163-174. http://dx.doi.org/10.2478/acph-2021-0016 PMID: 33151166

[25] Daoud, S.; Abutayeh, R.; Alabed, S.J.; Taha, M.O. Asenapine as a Potential Lead Inhibitor against Central Ca2+/Calmodulin-Dependent Protein Kinase II: Investigation by Docking Simulation and Experimental Validation. *Open Med. Chem. J.,* **2023**, *17*(1), 187410452301260. http://dx.doi.org/10.2174/18741045-v17-e230217-2022-14

[26] Z'-LYTE Kinase assay kits. Available from: https://www.thermofisher.com/jo/en/home/industrial/pharma-biopharma/drug-discovery-development/target-and-lead-identification-and-validation/kinasebiology/kinase-activity-assays/z-lyte.html

[27] Z'-LYTE Kinase Assay Technology. SelectScreen® Kinase Profiling Services. **2021**. Available from: https://documents.thermofisher.com/TFS-Assets/BID/Scientific-Resources/ssbk-customer-protocol-and-assay-conditions.pdf

[28] Ma, H.; Deacon, S.; Horiuchi, K. The challenge of selecting protein kinase assays for lead discovery optimization. *Expert Opin. Drug Discov.,* **2008**, *3*(6), 607-621. http://dx.doi.org/10.1517/17460441.3.6.607 PMID: 19662101

[29] Cowan-Jacob, S.W.; Möbitz, H.; Fabbro, D. Structural biology contributions to tyrosine kinase drug discovery. *Curr. Opin. Cell Biol.,* **2009**, *21*(2), 280-287. http://dx.doi.org/10.1016/j.ceb.2009.01.012 PMID: 19208462

[30] Ghasemi, M.; Liang, S.; Luu, Q.M.; Kempson, I. The MTT assay: A method for error minimization and interpretation in measuring cytotoxicity and estimating cell viability. *Methods Mol. Biol.,* **2023**, *2644*, 15-33. http://dx.doi.org/10.1007/978-1-0716-3052-5_2 PMID: 37142913

[31] Stockert, J.C.; Horobin, R.W.; Colombo, L.L.; Blázquez-Castro, A. Tetrazolium salts and formazan products in Cell Biology: Viability assessment, fluorescence imaging, and labeling perspectives. *Acta Histochem.,* **2018**, *120*(3), 159-167. http://dx.doi.org/10.1016/j.acthis.2018.02.005 PMID: 29496266

[32] Jin, H.; Zhang, C.; Zwahlen, M.; von Feilitzen, K.; Karlsson, M.; Shi, M.; Yuan, M.; Song, X.; Li, X.; Yang, H.; Turkez, H.; Fagerberg, L.; Uhlén, M.; Mardinoglu, A. Systematic transcriptional analysis of human cell lines for gene expression landscape and tumor representation. *Nat. Commun.,* **2023**, *14*(1), 5417. http://dx.doi.org/10.1038/s41467-023-41132-w PMID: 37669926

[33] Mader, M.M. Which small molecule? Selecting chemical probes for cancer research. *Cancer Discov.,* **2023**, *13*(10), 2150-2165. http://dx.doi.org/10.1158/2159-8290.CD-23-0536 PMID: 37712569

[34] Diller, D.J.; Merz, K.M., Jr High throughput docking for library design and library prioritization. *Proteins,* **2001**, *43*(2), 113-124. http://dx.doi.org/10.1002/1097-0134(20010501)43:2<113::AID-PROT1023>3.0.CO;2-T PMID: 11276081

[35] Rao, S.N.; Head, M.S.; Kulkarni, A.; LaLonde, J.M. Validation studies of the site-directed docking program LibDock. *J. Chem. Inf. Model.,* **2007**, *47*(6), 2159-2171. http://dx.doi.org/10.1021/ci6004299 PMID: 17985863

[36] Jain, A.N. Scoring noncovalent protein-ligand interactions: A continuous differentiable function tuned to compute binding affinities. *J. Comput. Aided Mol. Des.,* **1996**, *10*(5), 427-440. http://dx.doi.org/10.1007/BF00124474 PMID: 8951652

[37] Krammer, A.; Kirchhoff, P.D.; Jiang, X.; Venkatachalam, C.M.; Waldman, M. LigScore: A novel scoring function for predicting binding affinities. *J. Mol. Graph. Model.,* **2005**, *23*(5), 395-407. http://dx.doi.org/10.1016/j.jmgm.2004.11.007 PMID: 15781182

[38] Chen, C.Y.C. Weighted equation and rules--a novel concept for evaluating protein-ligand interaction. *J. Biomol. Struct. Dyn.,* **2009**, *27*(3), 271-282. http://dx.doi.org/10.1080/07391102.2009.10507315 PMID: 19795911

[39] Šinko, G. Assessment of scoring functions and *in silico* parameters for AChE-ligand interactions as a tool for predicting inhibition potency. *Chem. Biol. Interact.,* **2019**, *308*, 216-223. http://dx.doi.org/10.1016/j.cbi.2019.05.047 PMID: 31150627

[40] Ramírez, D.; Caballero, J. Is it reliable to take the molecular docking top scoring position as the best solution? *Molecules,* **2018**, *23*(5), 1038. http://dx.doi.org/10.3390/molecules23051038 PMID: 29710787

[41] Hevener, K.E.; Zhao, W.; Ball, D.M.; Babaoglu, K.; Qi, J.; White, S.W.; Lee, R.E. Validation of molecular docking programs for virtual screening against dihydropteroate synthase. *J. Chem. Inf. Model.,* **2009**, *49*(2), 444-460. http://dx.doi.org/10.1021/ci800293n PMID: 19434845

[42] Pagadala, N.S.; Syed, K.; Tuszynski, J. Software for molecular docking: A review. *Biophys. Rev.,* **2017**, *9*(2), 91-102. http://dx.doi.org/10.1007/s12551-016-0247-1 PMID: 28510083

[43] Blanes-Mira, C.; Fernández-Aguado, P.; de Andrés-López, J.; Fernández-Carvajal, A.; Ferrer-Montiel, A.; Fernández-Ballester, G. Comprehensive survey of consensus docking for high-throughput virtual screening. *Molecules,* **2022**, *28*(1), 175. http://dx.doi.org/10.3390/molecules28010175 PMID: 36615367

[44] Charifson, P.S.; Corkery, J.J.; Murcko, M.A.; Walters, W.P. Consensus scoring: A method for obtaining improved hit rates from docking databases of three-dimensional structures into proteins. *J. Med. Chem.,* **1999**, *42*(25), 5100-5109. http://dx.doi.org/10.1021/jm990352k PMID: 10602695

[45] Cumming, G. Inference by eye: Reading the overlap of independent confidence intervals. *Stat. Med.,* **2009**, *28*(2), 205-220. http://dx.doi.org/10.1002/sim.3471 PMID: 18991332

[46] Islam, S.; Wang, S.; Bowden, N.; Martin, J.; Head, R. Repurposing existing therapeutics, its importance in oncology drug development: Kinases as a potential target. *Br. J. Clin. Pharmacol.,* **2022**, *88*(1), 64-74. http://dx.doi.org/10.1111/bcp.14964 PMID: 34192364

[47] Sen, S.; Kushwah, H.; Ranjan, O.P. Drug Repurposing in Cancer Therapy. In: *Drug Repurposing*; Chella, N.; Ranjan, O.P.; Alexander, A., Eds.; Springer: Singapore, **2024**; pp. 57-92. http://dx.doi.org/10.1007/978-981-97-5016-0_5

[48] Shoichet, B.K. Interpreting steep dose-response curves in early inhibitor discovery. *J. Med. Chem.,* **2006**, *49*(25), 7274-7277. http://dx.doi.org/10.1021/jm061103g PMID: 17149857

[49] Rikitake, Y.; Kim, H.H.; Huang, Z.; Seto, M.; Yano, K.; Asano, T.; Moskowitz, M.A.; Liao, J.K. Inhibition of Rho kinase (ROCK) leads to increased cerebral blood flow and stroke protection. *Stroke,* **2005**, *36*(10), 2251-2257. http://dx.doi.org/10.1161/01.STR.0000181077.84981.11 PMID: 16141422

[50] Uehata, M.; Ishizaki, T.; Satoh, H.; Ono, T.; Kawahara, T.; Morishita, T.; Tamakawa, H.; Yamagami, K.; Inui, J.; Maekawa, M.; Narumiya, S. Calcium sensitization of smooth muscle mediated by a Rho-associated protein kinase in hypertension. *Nature,* **1997**, *389*(6654), 990-994. http://dx.doi.org/10.1038/40187 PMID: 9353125

[51] Garnock-Jones, K.P. Ripasudil: First global approval. *Drugs,* **2014**, *74*(18), 2211-2215. http://dx.doi.org/10.1007/s40265-014-0333-2 PMID: 25414122

[52] Zanin-Zhorov, A.; Weiss, J.M.; Nyuydzefe, M.S.; Chen, W.; Scher, J.U.; Mo, R.; Depoil, D.; Rao, N.; Liu, B.; Wei, J.; Lucas, S.; Koslow, M.; Roche, M.; Schueller, O.; Weiss, S.; Poyurovsky, M.V.; Tonra, J.; Hippen, K.L.; Dustin, M.L.; Blazar, B.R.; Liu, C.; Waksal, S.D. Selective oral ROCK2 inhibitor down-regulates IL-21 and IL-17 secretion in human T cells *via* STAT3-dependent mechanism. *Proc. Natl. Acad. Sci. USA,* **2014**, *111*(47), 16814-16819. http://dx.doi.org/10.1073/pnas.1414189111 PMID: 25385601

[53] Jagasia, M.; Lazaryan, A.; Bachier, C.R.; Salhotra, A.; Weisdorf, D.J.; Zoghi, B.; Essell, J.; Green, L.; Schueller, O.; Patel, J.; Zanin-Zhorov, A.; Weiss, J.M.; Yang, Z.; Eiznhamer, D.; Aggarwal, S.K.; Blazar, B.R.; Lee, S.J. ROCK2 inhibition with belumosudil (KD025) for the treatment of chronic graft-versus-host disease. *J. Clin. Oncol.,* **2021**, *39*(17), 1888-1898. http://dx.doi.org/10.1200/JCO.20.02754 PMID: 33877856

[54] Dobutamine. **2025**. Available from: https://pubchem.ncbi.nlm.nih.gov/compound/Dobutamine

[55] Julian, L.; Olson, M.F. Rho-associated coiled-coil containing kinases (ROCK): Structure, regulation, and functions. *Small GTPases,* **2014**, *5*(2), 29846. http://dx.doi.org/10.4161/sgtp.29846 PMID: 25010901

[56] Kinnings, S.L.; Liu, N.; Tonge, P.J.; Jackson, R.M.; Xie, L.; Bourne, P.E. A machine learning-based method to improve docking scoring functions and its application to drug repurposing. *J. Chem. Inf. Model.,* **2011**, *51*(2), 408-419. http://dx.doi.org/10.1021/ci100369f PMID: 21291174

[57] Guedes, I.A.; Pereira, F.S.S.; Dardenne, L.E. Empirical scoring functions for structure-based virtual screening: Applications, critical aspects, and challenges. *Front. Pharmacol.,* **2018**, *9*, 1089. http://dx.doi.org/10.3389/fphar.2018.01089 PMID: 30319422

[58] Li, Y.; Han, L.; Liu, Z.; Wang, R. Comparative assessment of scoring functions on an updated benchmark: 2. Evaluation methods and general results. *J. Chem. Inf. Model.,* **2014**, *54*(6), 1717-1736. http://dx.doi.org/10.1021/ci500081m PMID: 24708446

[59] Copeland, R.A. Biochemical assay conditions and their influence on measured IC50 values. In: *Evaluation of enzyme inhibitors in drug discovery: A guide for medicinal chemists and pharmacologists*; Wiley: Hoboken, **2013**. http://dx.doi.org/10.1002/9781118540398

[60] Gehlhaar, D.K.; Verkhivker, G.M.; Rejto, P.A.; Sherman, C.J.; Fogel, D.R.; Fogel, L.J.; Freer, S.T. Molecular recognition of the inhibitor AG-1343 by HIV-1 protease: Conformationally flexible docking by evolutionary programming. *Chem. Biol.,* **1995**, *2*(5), 317-324. http://dx.doi.org/10.1016/1074-5521(95)90050-0 PMID: 9383433

[61] You, Y.; Zhu, K.; Wang, J.; Liang, Q.; Li, W.; Wang, L.; Guo, B.; Zhou, J.; Feng, X.; Shi, J. ROCK inhibitor: Focus on recent updates. *Chin. Chem. Lett.,* **2023**, *34*(12), 108336. http://dx.doi.org/10.1016/j.cclet.2023.108336

[62] Anastassiadis, T.; Duong-Ly, K.C.; Deacon, S.W.; Lafontant, A.; Ma, H.; Devarajan, K.; Dunbrack, R.L., Jr; Wu, J.; Peterson, J.R. A highly selective dual insulin receptor (IR)/insulin-like growth factor 1 receptor (IGF-1R) inhibitor derived from an extracellular signal-regulated kinase (ERK) inhibitor. *J. Biol. Chem.,* **2013**, *288*(39), 28068-28077. http://dx.doi.org/10.1074/jbc.M113.505032 PMID: 23935097

[63] Defert, O.; Boland, S. Rho kinase inhibitors: A patent review (2014 - 2016). *Expert Opin Ther Pat,* **2017**, *27*(4), 507-515. http://dx.doi.org/10.1080/13543776.2017.1272579 PMID: 28048944

[64] Zhao, Z.; Bourne, P.E. How ligands interact with the kinase hinge. *ACS Med. Chem. Lett.,* **2023**, *14*(11), 1503-1508. http://dx.doi.org/10.1021/acsmedchemlett.3c00212 PMID: 37974950

[65] Beljkas, M.; Petkovic, M.; Vuletic, A.; Djuric, A.; Santibanez, J.F.; Srdic-Rajic, T.; Nikolic, K.; Oljacic, S. Development of Novel ROCK Inhibitors *via* 3D-QSAR and Molecular Docking Studies: A Framework for Multi-Target Drug Design. *Pharmaceutics,* **2024**, *16*(10), 1250. http://dx.doi.org/10.3390/pharmaceutics16101250 PMID: 39458584

[66] Xing, L.; Klug-Mcleod, J.; Rai, B.; Lunney, E.A. Kinase hinge binding scaffolds and their hydrogen bond patterns. *Bioorg. Med. Chem.,* **2015**, *23*(19), 6520-6527. http://dx.doi.org/10.1016/j.bmc.2015.08.006 PMID: 26358279

[67] Klebe, G.; Böhm, H.J. Energetic and entropic factors determining binding affinity in protein-ligand complexes. *J. Recept. Signal Transduct. Res.,* **1997**, *17*(1-3), 459-473. http://dx.doi.org/10.3109/10799899709036621 PMID: 9029508

[68] Daoud, S.; Taha, M.O. Design and synthesis of new JAK1 inhibitors based on sulfonamide-triazine conjugates. *Curr. Computeraided Drug Des.,* **2021**, *17*(7), 916-926. http://dx.doi.org/10.2174/1573409916666201224152253 PMID: 33357183

[69] Daoud, S.; Thiab, S.; Jazzazi, T.M.A.; Al-Shboul, T.M.A.; Ullah, S. Evaluation and molecular modelling of bis-Schiff base derivatives as potential leads for management of diabetes mellitus. *Acta Pharm.,* **2022**, *72*(3), 449-458. http://dx.doi.org/10.2478/acph-2022-0019 PMID: 36651543

[70] Abudayah, A.; Daoud, S.; Al-Sha'er, M.A.; Omar Taha, M. Pharmacophore modeling of targets infested with activity cliffs *via* molecular dynamics simulation coupled with QSAR and comparison with other pharmacophore generation methods: KDR as case study. *Mol. Inform.,* **2022**, *41*(11), 2200049. http://dx.doi.org/10.1002/minf.202200049 PMID: 35973966

[71] Nitulescu, G.M.; Stancov, G.; Seremet, O.C.; Nitulescu, G.; Mihai, D.P.; Duta-Bratu, C.G.; Barbuceanu, S.F.; Olaru, O.T. The importance of the pyrazole scaffold in the design of protein kinases inhibitors as targeted anticancer therapies. *Molecules,* **2023**, *28*(14), 5359. http://dx.doi.org/10.3390/molecules28145359 PMID: 37513232

[72] Pantziarka, P.; Bouche, G.; Sukhatme, V.; Meheus, L.; Rooman, I.; Sukhatme, V.P. Repurposing Drugs in Oncology (ReDO)-Propranolol as an anti-cancer agent. *Ecancermedicalscience,* **2016**, *10*, 680. http://dx.doi.org/10.3332/ecancer.2016.680 PMID: 27899953

[73] Ma, Z.; Liu, X.; Zhang, Q.; Yu, Z.; Gao, D. Carvedilol suppresses malignant proliferation of mammary epithelial cells through inhibition of the ROS-mediated PI3K/AKT signaling pathway. *Oncol. Rep.,* **2018**, *41*(2), 811-818. http://dx.doi.org/10.3892/or.2018.6873 PMID: 30483797

[74] Regulska, K.; Regulski, M.; Karolak, B.; Murias, M.; Stanisz, B. Can cardiovascular drugs support cancer treatment? The rationale for drug repurposing. *Drug Discov. Today,* **2019**, *24*(4), 1059-1065. http://dx.doi.org/10.1016/j.drudis.2019.03.010 PMID: 30878563